

Influence of Phonon dimensionality on Electron Energy Relaxation

J.T. Karvonen and I.J. Maasilta

Nanoscience Center, Department of Physics, P.O. Box 35, FIN-40014 University of Jyväskylä, Finland.

We studied experimentally the role of phonon dimensionality on electron-phonon (e-p) interaction in thin copper wires evaporated either on suspended silicon nitride membranes or on bulk substrates, at sub-Kelvin temperatures. The power emitted from electrons to phonons was measured using sensitive normal metal-insulator-superconductor (NIS) tunnel junction thermometers. Membrane thicknesses ranging from 30 nm to 750 nm were used to clearly see the onset of the effects of two-dimensional (2D) phonon system. We observed for the first time that a 2D phonon spectrum clearly changes the temperature dependence and strength of the e-p scattering rate, with the interaction becoming stronger at the lowest temperatures below ~ 0.5 K for the 30 nm membranes.

PACS numbers: 63.22.+m, 63.20.Kr, 85.85.+j

It is an established fact that at sub-Kelvin temperatures the thermal coupling between conduction electrons and the lattice becomes very weak [1]. This has significant implications for the operation of low-temperature detectors and coolers [2], or for any solid-state systems where dissipation and cooling are relevant. Low-temperature electron-phonon (e-p) interaction has been studied widely during the past decades, but mostly only for the case in which the phonons are fully three dimensional (3D) [3, 4, 5, 6]. However, due to significant advances in fabrication of thin suspended structures, many practical devices and detectors exist in which the phonons are expected to move freely only within the plane of a membrane, forming a quasi-2D system [7]. The question how the two-dimensionality of the phonon modes influences e-p interaction has been addressed theoretically for certain cases [8, 9, 10], but no clear experimental observation of the effect has been reported to date, although several attempts have been made [11, 12].

In this paper, we show for the first time experimentally that the electron-phonon interaction clearly changes depending on the dimensionality of the phonons, as expected from theory. E-p coupling was measured with the help of sensitive NIS tunnel junction thermometry [13], for thin Cu wires on suspended silicon nitride (SiN_x) membranes with thickness varying from 30 nm to 750 nm, which spans the transition from 2D to 3D phonons. In addition, samples with identical Cu wires on bulk substrates were also measured for comparison. For the thinnest membranes, the e-p interaction was *strengthened* in comparison with the bulk samples, and its temperature dependence changed significantly, as is predicted by the theory [8, 9, 10]. The change was large enough to give indirect evidence that the dispersive ($\omega \sim k^2$), flexural modes of the membrane play a major role in the e-p interaction.

In the presence of stress-free boundaries, the bulk transversal and longitudinal phonon modes (with sound velocities c_t and c_l , respectively) couple to each other and form a new set of eigenmodes, which in the case of a suspended membrane are known as the horizontal shear modes (h), and symmetric (s) and antisymmetric (a) Lamb modes [14]. The frequency ω for the h

modes is simply $\omega = c_t \sqrt{k_{\parallel}^2 + (m\pi/d)^2}$, where k_{\parallel} is the wave vector component parallel to the membrane surfaces, d is the membrane thickness and the integer m is the branch number. However, the dispersion relations of the s and a Lamb modes cannot be given in a closed analytical form, but have to be calculated numerically. The lowest three branches, dominant for thin membranes at low temperatures, have low frequency analytical expressions: $\omega_h = c_t k_{\parallel}$, $\omega_s = c_s k_{\parallel}$, and $\omega_a = \frac{\hbar}{2m^*} k_{\parallel}^2$, where $c_s = 2c_t \sqrt{(c_l^2 - c_t^2)/c_l^2}$ is the effective sound velocity of the s mode, and $m^* = \hbar \left[2c_t d \sqrt{(c_l^2 - c_t^2)/3c_l^2} \right]^{-1}$ is an effective mass for the a -mode "particle". This lowest a -mode with its quadratic dispersion is mostly responsible for the non-trivial behavior of the e-p interaction [9, 10]. Note that already a single free surface affects the modes [15] and the e-p interaction [16], as the bulk modes couple and form another new set of eigenstates, including the surface localized Rayleigh-mode. Thus, the widely observed result for e-p power flow $P = \Sigma V(T_e^5 - T_p^5)$ from a metal volume V with T_e the electron and T_p the phonon temperature, is not expected to hold even for thin enough films on bulk substrates.

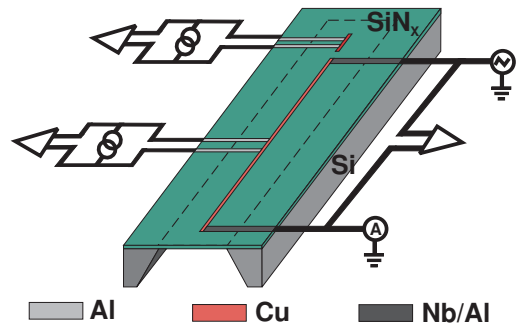


FIG. 1: (Color online) A Schematic of the suspended samples and the measuring circuit. Red lines are the normal metal Cu, light gray Al for SINIS-junctions and dark gray Al or Nb for SN-junctions.

A schematic of the Cu wire samples on suspended silicon nitride membranes and the used measuring circuit

is shown in Fig. 1. 17 samples were made on either suspended membranes or bulk substrates, where nitridized (100) Si wafers with 30, 200 and 750 nm thick low-stress SiN_x top layers were used as the substrate for both cases. The suspension of the SiN_x membranes (size $600 \times 300 \mu\text{m}^2$) was achieved by anisotropic backside wet etching of the silicon substrate in KOH, and the metallic structures were fabricated using standard e-beam lithography and multi-angle shadow mask evaporation techniques. As the e-p interaction strength is sensitive to the thickness and disorder level of the metal [17], we minimized its effect by evaporating the Cu wires of a specific thickness on all the different substrates simultaneously. Ultrathin Cu layers ($t=14\text{-}30$ nm) were used to strengthen the effect of the thin membranes. The oxide layer forming the tunnel junction barriers was produced by thermal oxidation of Al. Table I presents the essential dimensions of the samples discussed in this paper, measured by scanning electron (SEM) and atomic force (AFM) microscopies. The electron mean free path was determined from the resistance of the wire at base temperature 60 mK, using the accurately measured dimensions of the wire.

TABLE I: Parameters for samples. M= suspended SiN_x membrane and B= bulk substrate. B6 had an oxidized Si substrate.

Sample	SiN_x d (nm)	Cu t (nm)	V [(μm) ³]	l (nm)	$\tau(0.2\text{K})$ (μs)	$\tau(0.8\text{K})$ (μs)
M1	30	14	2.71	5.7	2.6	0.16
B1	30	14	2.46	4.9	7.1	0.030
M2	200	14	2.44	4.6	15.0	0.11
B2	200	18	3.67	4.1	6.4	0.045
M3	30	19	5.50	11.2	2.2	0.30
B3	30	19	4.62	9.8	4.3	0.034
M4	750	22	6.09	10.3	3.1	0.030
B4	750	22	5.87	8.7	3.9	0.013
M5	30	32	6.09	22	1.8	0.31
B5	30	32	5.09	19	2.7	0.038
B6	-	32	7.10	22	1.6	0.031

We used the hot-electron technique [3] to measure the e-p interaction by overheating the electrons by Joule heat power P and measuring the resulting electron temperature T_e . All the samples had two electrically isolated Cu normal metal wires next to each other. The longer wire ($L = 500 \mu\text{m}$) was heated by applying a slowly ramping voltage across the pair of superconducting Nb (or Al) leads in direct metallic contact to Cu, forming SN junctions. These junctions provide excellent electrical, but very poor thermal conductance due to Andreev reflection, as the junctions are biased within the superconducting gap Δ . Thus, due to the lack of outdiffusion of electrons and the long length of the wire, input heat is distributed uniformly in the interior of the wire and the electron gas cools dominantly by phonons, instead of diffusively [18] or by thermal photons [19]. Since $L \gg L_{e-e}$, the electron-electron scattering length, electron temperature is also well defined without complica-

tions from non-equilibrium [20]. In our sample geometry the electron temperature is measured with two additional Al leads forming a NIS tunnel junctions pair (SINIS) in the middle of heated wire, as a function of input Joule power $P = IV$ measured in a four probe configuration. The purpose of the short Cu wire, with additional SINIS thermometer on it, is to give an estimate of the local phonon temperature T_p , as the e-p power flow depends on both T_e and T_p .

The current-biased Al SINIS thermometer is ideally suited to measure temperature below a few Kelvins, [2] due to its high sensitivity (in our DC measurement ~ 0.1 mK at 0.1 K) and low power dissipation. In addition, for all the data here, the SINIS voltage vs. temperature response follows the BCS theory without fitting parameters very accurately at least down to ~ 0.2 K, where typically saturation sets in. This saturation depends on the strength of the e-p interaction (size of thermometer and type of substrate) and the amount of filtering, and thus we conclude that it is most likely caused by external noise heating. For this reason we take the most conservative approach and assume that all saturation is caused by it, in which case we can use the BCS theory to convert our voltage data for all temperatures.

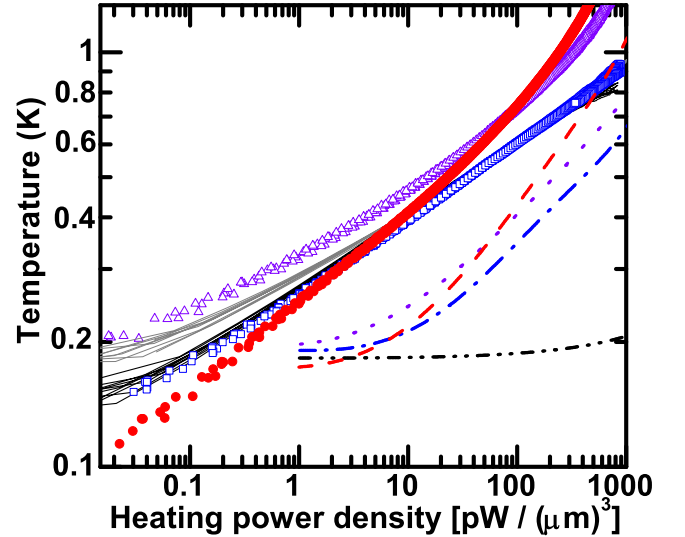


FIG. 2: (Color online) Measured electron and phonon temperatures T_e and T_p versus the applied heating power density in log-log-scale. Red, solid dots: T_e of sample M1 ($d = 30$ nm). Violet open triangles: T_e of sample M2 ($d = 200$ nm). Blue open squares: T_e of sample M4 ($d = 750$ nm). Gray line: T_e of samples B1 and B2. Black line: T_e of sample B4. Red dashed line: T_p of sample M3. Violet dotted line: T_p of M2. Blue dash-dotted line: T_p of M4. Black dash-dot-dot line: T_p for all bulk samples.

Even if the electrons lose their energy overwhelmingly to the phonons in our sample geometry, it is still possible that the measured temperature is not only determined by the e-p interaction. This is because the emitted phonons could scatter so strongly that the phonon transmission

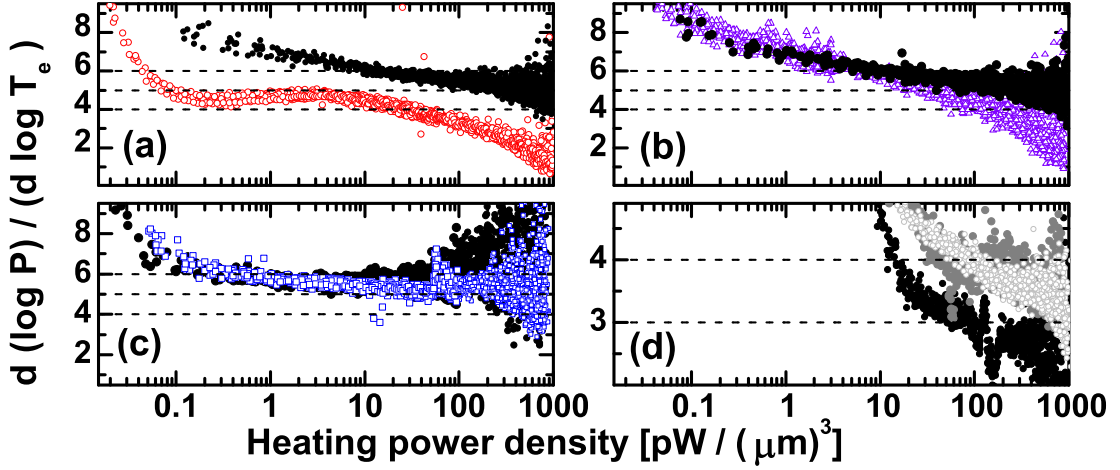


FIG. 3: (Color online) Numerical logarithmic derivatives of the measured data in Fig. 2. (a) T_e data. Red open circles: sample M1. Black solid dots: sample B1. (b) T_e data. Violet open triangles: sample M2. Black solid dots: sample B2. (c) T_e data. Blue open squares: M4. Black solid dots: sample B4. (d) T_p data. Black solid dots: sample M3. Light gray open circles: sample M4. Gray solid dots: sample M4.

becomes a bottleneck for the energy flow. Bulk scattering of phonons at low temperatures is very weak [7], even for thin disordered membranes [21]. However, boundary (or Kapitza) scattering can become significant, if the discontinuity of the elastic parameters is large enough. For thin films on bulk substrates, the effect of boundary resistance has been studied extensively [22], with the result that it is estimated to be small below ~ 1 K for the materials and film thicknesses used in this work (maximum 1-5 % effect for T_e at 1 K for $t = 15..30$ nm). In contrast, almost nothing quantitative is known about the boundary resistance between a thin metal film and a thin 2D membrane, or between a thin 2D membrane and a bulk substrate. However, it seems clear that if the combined metal film and membrane thickness is below the thermal wavelength of the phonons, the phonon modes in the two materials are strongly coupled, leading to an effectively non-existent boundary resistance. [23] Hence, if we check that the membrane temperature T_p is not too high compared to T_e (effects of the membrane-bulk boundary resistance and/or the scattering in the membrane), we can be confident that the measured T_e reflects the e-p interaction.

Figure 2 shows the main result of the measurements, with T_e and T_p plotted vs. the heating power density P/V for all membrane thicknesses (30 nm, 200 nm and 750 nm). In addition, data from a few representative bulk samples are shown. Compared to the corresponding bulk substrate sample (B4), T_e of the 750 nm membrane (M4) shows no difference at all, and it effectively behaves as bulk. This is reasonable, because for the 750 nm membrane the estimated dimensionality cross-over temperature [24, 25] $T_{cr} = \hbar c_t / (2k_B d)$ is ~ 30 mK, with $c_t = 6200$ m/s for SiN. The phonon temperatures T_p , however, show a big difference: The bulk samples shows almost no response from the saturation value of the ther-

mometer ~ 190 mK, whereas the membrane phonons heat up measurably, most likely due to the boundary resistance between the membrane and the bulk. Nevertheless, this increase in T_p for sample M4 is small enough not to influence T_e . For the 200 nm thick membrane (M2) ($T_{cr} \sim 110$ mK), at low heating power densities [$P/V < 40$ pW/(μm)³] the temperature dependence follows the behavior of the bulk sample (B2), although with a difference in the absolute value. This shows that the strength of the e-p coupling weakens compared to the bulk. At higher powers and temperatures ($P/V > 40$ pW/(μm)³, where $T_e > 0.6$ K), T_e starts to increase more rapidly in the membrane sample, most likely due to the boundary resistance effects. The phonons in the 30 nm thick membrane sample (M1) are expected to be in the 2D limit at low temperatures ($T_{cr} \sim 0.5$ K), and a clear sign of this can be seen in Fig. 2 as a strongly different behavior of the measured T_e vs. P/V curve with respect to all other samples. Below ~ 6 pW/(μm)³ the e-p coupling is notably stronger (T_e lower) than in the corresponding bulk (B1) or any other sample, but again at highest temperatures the influence of other effects starts to dominate over the e-p coupling.

To study the temperature dependence of the data in Fig. 2 more accurately, we plot the logarithmic derivatives $d(\log P/V)/d(\log T_e)$ in Fig. 3 (a)-(c). For low heating powers ($T_e^n \gg T_p^n$) $P_{e-p} \approx T_e^n$, where n is the power law of the e-p interaction, thus in that regime $d(\log P/V)/d(\log T_e) = n$. Typically this exponent is $n \approx 5$ for thicker ($t > 30$ nm) metal films on bulk substrates [3, 4, 17], if the disorder in the film is not too strong [26, 27, 28]. From Fig. 3 (a) we first of all see that for the 30 nm membrane sample M1, the difference to the bulk sample B1 is very clear. The M1 data has a plateau of $n \sim 4.5$ between $P/V = 0.1 - 6$ pW/(μm)³, while for B1, n continuously decreases from much higher values.

Note that the strong increase of $d(\log P/V)/d(\log T_e)$ below $P/V \sim 0.1 \text{ pW}/(\mu\text{m})^3$ is caused by the saturation of the T_e measurement, and not by the e-p interaction. The point where n starts deviating from $n = 4.5$ corresponds to $T_e \approx 0.4 \text{ K}$, which is surprisingly consistent with the estimated $T_{cr} \sim 0.5 \text{ K}$. In contrast, the temperature dependence of the 200 nm membrane (M2) and bulk (B2) samples [Fig. 3 (b)] are identical with each other and with the 30 nm bulk sample (B1), as long as the e-p interaction is dominant (up to $40 \text{ pW}/(\mu\text{m})^3$). The 750 nm membrane (M4) and bulk (B4) samples also give identical values of n [Fig. 4 (c)]. The difference between samples M4,B4 and M2,B2 is caused by the Cu wire thickness, which is expected to influence the temperature dependence strongly [16, 27].

We have also plotted the logarithmic derivatives for the membrane phonon data in Fig. 3 (d). It is interesting to see that the temperature dependence of T_p also changes with the phonon dimensionality, from $n \sim 4$ in the 3D limit to $n \sim 3$, consistent with the T_e data. The observed exponent in the 3D limit is in agreement with the theory for the boundary resistance for 3D systems, $P \sim T^4$. For the 2D-3D case no calculations are known to the authors.

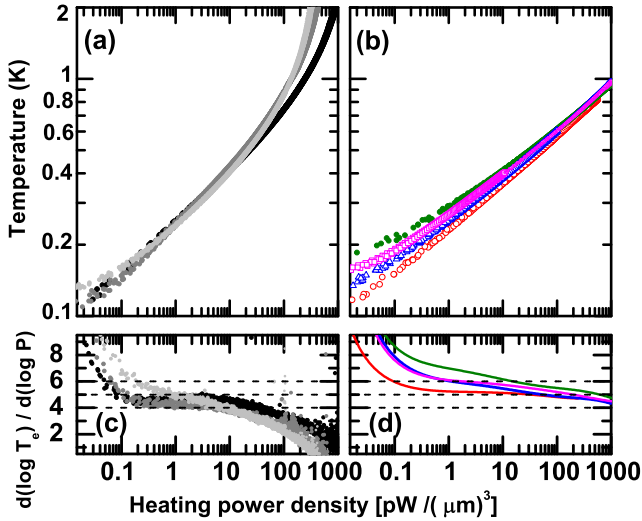


FIG. 4: (Color online) (a) T_e versus P/V for 30 nm membrane samples. Black solid dots: sample M1. Gray solid dots: sample M3. Light gray solid dots: sample M5. (b) T_e versus P/V for bulk samples. From top to bottom, Green solid dots: sample B1 (top). Magenta open squares: sample B3. Blue open triangles: sample B5. Red open circles: sample B6 (bottom). (c) Numerical logarithmic derivatives of the measured data in (a). Symbols are explained above. (d) Numerical logarithmic derivatives of the data in (b). From top to bottom, Green line: sample B1 (top). Magenta line: sample B3. Blue line: sample B5. Red line: sample B6 (bottom). Noise has been removed to help the eye.

Finally, we discuss the effect of the Cu wire thickness on the measured e-p interaction. The results for the thinnest 30 nm membrane samples, with Cu thickness $t = 14, 19$ and 32 nm are shown in Figs 4 (a) and (c). It is apparent that the metal film thickness has only a minor effect on the e-p interaction on thin membranes, and only influences the boundary resistance, by increasing its effect for thicker t , as expected. However, for wires on bulk substrates, Figs 4 (b) and (d), the effect of the Cu wire thickness on e-p interaction is more profound. The thinner the Cu film, the more its temperature dependence deviates from $n = 5$, which, for comparison, is observed for a more typical $t = 32 \text{ nm}$ Cu wire on oxidized Si (B6). This behavior is qualitatively consistent with the predicted effect of the surface phonon modes [16], but could also depend on the disorder, as the thickening of the film increases the mean free path l (Table I) and pushes the sample closer to the clean limit. An apparent exponent as high as ~ 7 could possibly be explained by the combination of strong disorder and surface modes, but again, detailed theory is lacking.

In conclusion, we have obtained the first clear evidence that the electron-phonon interaction at low temperatures changes quite significantly when the phonon modes become two-dimensional. To quantify the effects, the electron thermal relaxation times $\tau = \gamma V T_e / (dP/dT_e)$, where $\gamma = 100 \text{ J/K}^2\text{m}^3$ for Cu, are presented in Table I for all the samples at two temperatures $T_e = 0.2$ and 0.8 K . At $T_e < 0.5 \text{ K}$, the thinnest membranes can have a factor 2-3 strengthening effect, whereas at higher temperatures the thermal relaxation from membranes can be an order of magnitude weaker compared to bulk samples. The membrane close to transition region ($d=200 \text{ nm}$) was shown to have a weaker (\sim factor of two) e-p interaction strength than the bulk samples. Thinning the metal film on bulk substrates also leads to a sizeable weakening of the e-p interaction. The observed power law exponent for the 2D limit is consistent with $n \approx 4.5$, and is much smaller than the corresponding bulk exponent $n = 6..7$. A reduction by more than a factor one gives indirect evidence of the importance of the flexural, dispersive Lamb-modes for the membrane electron-phonon interaction, in agreement with theory [9, 10].

Discussions with T. Kühn and A. Sergeev are acknowledged. This work was supported by the Academy of Finland project Nos. 118665 and 118231.

- and J. P. Pekola, Rev. Mod. Phys. **78**, 217 (2006).
- [3] M. L. Roukes, M. R. Freeman, R. S. Germain, R. C. Richardson, and M. B. Ketchen, Phys. Rev. Lett. **55**, 422 (1985).
 - [4] F. C. Wellstood, C. Urbina, and J. Clarke, Phys. Rev. B **49**, 5942 (1994).
 - [5] M. Kanskär and M. N. Wybourne, Phys. Rev. Lett. **73**, 2123 (1994).
 - [6] D. R. Schmidt, C. S. Yung, and A. N. Cleland, Phys. Rev. B **69**, 140301 (2004).
 - [7] A. N. Cleland, *Foundations of Nanomechanics*, Springer, Berlin (2003).
 - [8] D. Belitz and S. Das Sarma, Phys. Rev. B **36**, 7701 (1987).
 - [9] K. Johnson, M. N. Wybourne and N. Perrin, Phys. Rev. B **50**, 2035 (1994).
 - [10] B. A. Glavin, V. I. Pipa, V. V. Mitin, and M. A. Strosio, Phys. Rev. B **65**, 205315 (2002).
 - [11] J. F. DiTusa, K. Lin, M. Park, M. S. Isaacson, and J. M. Parpia, Phys. Rev. Lett. **68**, 1156 (1992).
 - [12] Y. K. Kwong, K. Lin, M. S. Isaacson, and J. M. Parpia, J. Low Temp. Phys. **88**, 261 (1992).
 - [13] J. M. Rowell and D. C. Tsui, Phys. Rev. B **14**, 2456 (1976).
 - [14] B. A. Auld, *Acoustic Fields and Waves in Solids*, 2nd. Ed., Robert E. Krieger Publishing, Malabar, 1990.
 - [15] M. A. Geller, Phys. Rev. B **70**, 205421 (2004).
 - [16] S.-X. Qu, A. N. Cleland and M. R. Geller, Phys. Rev. B **72**, 224301 (2005).
 - [17] J. T. Karvonen, L. J. Taskinen and I. J. Maasilta, J. Low Temp. Phys. **146**, 213 (2007).
 - [18] C. Hoffmann, F. Lefloch, and M. Sanquer, Eur. Phys. J. B **29**, 629 (2002).
 - [19] M. Meschke, W. Guichard, and J. P. Pekola, Nature **444**, 187 (2006).
 - [20] H. Pothier, S. Guéron, Norman O. Birge, D. Esteve, and M. H. Devoret, Phys. Rev. Lett. **79**, 3490 (1997).
 - [21] T. Kühn, D.-V. Anghel, Y. M. Galperin, and M. Manninen, preprint.
 - [22] E. T. Swartz and R. O. Pohl, Rev. Mod. Phys. **61**, 605 (1989).
 - [23] The coupled modes would still scatter at the edge of the Cu wire, where the effective membrane thickness has a discontinuity.
 - [24] T. Kühn, D.-V. Anghel, J. P. Pekola, M. Manninen, and Y. M. Galperin, Phys. Rev. B **70**, 125425 (2004).
 - [25] T. Kühn and I. J. Maasilta, Nucl. Instrum. Methods Phys. Res. A **559**, 724 (2006); cond-mat/0702542.
 - [26] A. Schmid, Z. Phys. **259**, 421 (1973); in *Localization, Interaction and Transport Phenomena*, Springer 1985.
 - [27] M. Yu. Reizer and A. V. Sergeev, Zh. Eksp. Teor. Fiz. **90**, 1056 (1986) [Sov. Phys. JETP **63**, 616 (1986)]; A. Sergeev and V. Mitin, Phys. Rev. B **61**, 6041 (2000).
 - [28] L. J. Taskinen and I. J. Maasilta, Appl. Phys. Lett. **89**, 143511 (2006).